Biotechnology Reports 29 (2021) e00595

Contents lists available at ScienceDirect

Biotechnology Reports

journal homepage: www.elsevier.com/locate/btre

Research Article

Green synthesis of zinc oxide nanoparticles using leaf extracts of *Raphanus sativus var. Longipinnatus* and evaluation of their anticancer property in A549 cell lines

A. Umamaheswari*, S. Lakshmana Prabu, S. Adharsh John, A. Puratchikody

Department of Pharmaceutical Technology, University College of Engineering (BIT Campus), Anna University, Tiruchirappalli, 620 024, India

ARTICLE INFO

Article history:
Received 28 March 2020
Received in revised form 27 January 2021
Accepted 1 February 2021

Keywords:
Raphanus sativus var. Longipinnatus.
Green synthesis
Phytoconstituents
Zinc oxide nanoparticles
In vitro cytotoxicity
Lung cancer

ABSTRACT

In 21 st century, nanomedicine has turned out to be an emergent modulus operation for the diagnosis and treatment for cancer. The current study includes the Green synthesis of zinc oxide nanoparticles (ZnO NPs) from the leaves of *Raphanus sativus var. Longipinnatus* and interpretation of its anticancer activity. Synthesized ZnO NPs were investigated by UV–vis, FTIR, particle size analysis, SEM, XRD and its anticancer activity using A549 cell lines. The UV–vis and particle size confirmed the developed ZnO NPs are in nanoscale. The FTIR studies confirmed the presence of various functional groups. SEM and XRD pictures confirmed the partial crystal spherical shape and wurtzite crystal nature. The cytotoxicity results pointed out the enhanced cytotoxic effect of the synthesized ZnO NPs. This is the first attempt of *Raphanus sativus var. Longipinnatus* facilitated synthesis of ZnO NPs as anticancer agents and may subsequently be potential chemopreventive agent against other cancer treatment in future.

1. Introduction

Cancer has become primary cause of death among the human being and the treatment cost of it is also increasing drastically. Among the different cancers, the prevalence and death of men and women due to lung cancer is more common [1,2]. Despite the availability of easy diagnosis and treatment techniques such as chemically derived drugs, chemotherapy, surgery and radiotherapy, the patients suffer from severe side effects and induced strains due to the above treatment techniques [3]. Henceforth, researchers are focusing on the unique properties of nanomedicine as an alternative treatment technique for the verdict and treatment of cancer. The WHO estimated that nearly 75–80% of the global population still rely on their traditional medicinal practice for their health care requirements [4]. In 21st century, nanotechnology becomes an innovative field throughout the world in various fields. Nanoparticles (NPs) are traditionally synthesized by physical as well as chemical methods. Nowadays, green synthesis of NPs are much more accentuated among the researchers due to its considerable interest by evading toxic chemicals, high cost and severe reaction conditions [5]. Different biological sources like bacteria, fungi, yeast, actinobacteria, algae and plants are utilized for the green synthesis of NPs. Between the different biological sources, plants have been considered as the best candidate for the synthesis of metal NPs [6–9]. The reasons behind choosing the plant as a best candidate among the biological sources is that plants can provide a superior platform for the synthesis of nanoparticles over chemical and biological methods, free from toxic chemicals, feasibility in cost competitive, faster rate of synthesis, protective, secondary metabolites can act as natural reducing agent as well as capping agent, and the nanoparticles from plants materials are more stable than other biological sources [10–15].

There are several metal oxide NPs synthesized by green technology such as TiO_2 [16], Sm_2O_3 [17], Cr_2O_3 [18], NiO [19], CdO [20], Eu_2O_3 [21], SnO_2 [22], CuO [23], Fe_3O_4 [24] and ZnO [25]. Of these, zinc oxide nanoparticles (ZnO NPs) owe its unique physical and chemical properties which include adsorption of radiation, large excitation binding energy (60 meV), higher stability, wide band gap (~3.37 eV), electrochemical coupling coefficient, n-type semiconductivity, high rate of chemical reaction in presence of catalyst, inexpensive luminescent material non-toxic *etc.* [26]. Therefore, many researchers started to synthesis ZnO NPs and modify current ZnO NPs specially in controlling the particle shapes and particle size distribution. Generally, plant extract have many organic compound such as polyphenols, amino and carboxylic groups that have ability to take part in the synthesis of NPs by acting as reductants and stabilizer [27]. ZnO NPs

* Corresponding author.
E-mail address: umapharmaaut@gmail.com (A. Umamaheswari).

https://doi.org/10.1016/j.btre.2021.e00595

produced by plant can be obtained in a variety of shape and size with wide range of properties [28]. Furthermore, the properties of ZnO NPs react at the low processing temperature. Synthesis of ZnO NPs from plant is a simplest process, cheap, green and does not utilize any intermediate base group.

There are several researches where, the ZnO NPs were produced from the extracts of *Trifolium pretense* flower [29] *Nyctanthes arbor-tristis* flower [25] *Passiflora caerulea leaf extract* [30] *Catharanthus roseus* leafs [31] *Murraya koenigii* leaf [32] *Lathyrus sativus L. Root* [33] and *Aloe vera* leaf have proven enormous pharmacological activities by specific mechanistic actions [34].

The herb,*Raphanus sativus var. Longipinnatus* (*R. sativus* var. *Longipinnatus*)belongs to the family *Cruciferae*. It is a less dense hairy herb. Different leaf extracts of *Raphanus sativus var. Longipinnatus* were investigated for its activity and reported that it possesses antimicrobial, antioxidant, antitumor, antiviral, hypotensive and cardiovascular disease prevention activities [35]. In most of the countries, the leaves of *R. sativus* var. *Longipinnatus* has been eaten as food componentwhereas, in southern part of India especially in Tamil Nadu it has been often ignored and considered as waste and it is utilized as livestock feed. Based on the above review results, it is concluded that there is no investigation performed towards its anticancer activity. Bearing in mind of the facts like global need solid waste management and ecofriendly green synthesis approach, our specific aim of study was designed to green synthesis ZnO NPs using *Raphanus sativus var. Longipinnatus* leaves extract and evaluate its cytotoxic potential effect in A549 lung cancer cells.

2. Materials and methods

2.1. Plant materials

The specimen (*Raphanus sativus var. Longipinnatus* leaves) for the proposed study were collected from Tiruchirappalli District, Tamil Nadu, India and the specimen was confirmed by Dr.S. Soosairaj, Assistant Professor, Department of Botany, St. Joseph's College, Tiruchirappalli. Voucher specimens can be assessed as SJCBOT2182.

Organic solvents, Chemical reagents and chemicals are in Analytical Grade purchased from Sisco Research Laboratories Pvt. Ltd., India; analytical grade Zinc acetate dehydrate with the purity of 99.5% was purchased from Sisco Research Laboratories Pvt. Ltd., India.

2.2. Preparation of extract

Raphanus sativus var. Longipinnatus leaves (Fig. 1) were collected from fresh plant and removed the dust and foreign material by washing in tap water several times. Around 10 g of washed fine grinded leaves were taken in a 250 mL beaker having 100 mL of double distilled water and boiled in a water bath for 15 min. Subsequently, allowed the extract to cool until it attained the normal temperature, and then filtered through filter paper Whatman No.1. The filtrates were centrifuged at 10,000 rpm for 10 min, collected the supernatant and preserved at 4 °C. The same procedure was carried out for preparation of the dichloromethane and ethanol extracts. The supernatant extract was utilized for ZnO NPs synthesis.

2.3. Phytochemical analysis

All the three extracts were examined for its phytochemicals like flavonoids (ferric chloride test and lead acetate test), alkaloids (Mayers test and Hager's Test), tannins (gelatin test), saponins (Froth test), phenols (ferric chloride test), glycosides (Killer killiani test), protein (Biuret's test) and amino acid (ninhydrin test), phyto steroids (Salkowski's test), carbohydrates (Benedict's test), saponins (Froth test) and anthraquinones (Bontranger's Test) as per the earlier reported procedures [36].

2.3.1. Test for flavonoids

Alkaline reagent test - About 2 mL of the extract was added with few drops of 10% sodium hydroxide solution an intense yellow color formation indicates the presence of flavonoid.

Lead acetate test - About 2 mL of the extract was added with few drops of lead acetate solution, a yellow color precipitate formation indicates the presence of flavonoids.

2.3.2. Test for alkaloids

Mayer's Reagent – Extract of 1 mL was mixed with few drops of Mayer's reagent, a cream color precipitate formation indicates the presence of alkaloid.

About 3 mL of the extract was added to 1 mL of hydrochloric acid, mixed well and gently heated the mixture for 20 min, then cool to the room temperature. Subsequently the mixture was filtered through watt man filter paper. The filtrate was used for the following test.

Hager's test - About1 ml of the extract was mixed with few drops of Hager's reagent, a yellow color precipitate formation indicates the presence of Alkaloid.

2.3.3. Test for tannin

Gelatin test - About 2 mL of the extract was mixed with few drops of 10% and sodium chloride solution, a white buff color precipitate formation indicates the presence of tannin.

2.3.4. Test for phenol

Ferric chloride test - About 2 mL of the extract was mixed with few drops of 5% neutral ferric chloride solution, a dark green color formation indicates the presence of phenol.

2.3.5. Test for glycosides

Killer killiani test - About 2 mL of the extract was mixed with 2 mL of glacial acetic acid containing a drop of ferric chloride

Fig. 1. Leaves of the selected medicinal plant *Raphanus sativus var. Longipinnatus*.

solution, a brown color ring formation indicates the presence of glycoside.

2.3.6. Test for protein

Biuret's test - About 2 mL of the extract was mixed with few drops of 4% sodium hydroxide solution and 1% copper sulfate solution, formation of violet color indicates the presence of protein.

2.3.7. Test for amino acid

Ninhydrin test - About 2 mL of the extract was heated with 5% Ninhydrin solution, a violet color formation indicates the presence of amino acids.

2.3.8. Test for phyto steroids

Salkowski's test – Extract of 5 mL was treated with 2 mL of chloroform and few drops of concentrated sulphuric (H_2SO_4) acid was added in the side of the test tube, a reddish brown color formation indicates the presence of phyto-steroids.

2.3.9. Test for carbohydrates

About 2 mL of the extract was diluted with 5 mL of double distilled water, mixed well and followed by filtered. Then the filtrate was used to perform the Benedict's test.

Benedict's test: - Around 2 mL of filtrate was mixed with few drops of Benedict's reagent and gently heated; an orange red precipitate formation indicates the presence of carbohydrate.

2.3.10. Test for saponins

Froth test - About 1 mL of the extract was added with 3 mL of double distil1ed water and then the mixture was vigorously shaken, formation of foam indicates the presence of saponin.

2.3.11. Test for anthraquinones

Bontranger's Test- About 1 mL of the extract was mixed with 20 mL of chloroform, then heated for 5 min, filtered in hot condition and then allowed to cool to the room temperature. To the filterate equal volume of 10% ammonic solution was added and shaken well. Appearance of bright pink color in the aqueous layer indicates the presence of anthraquinones.

2.4. Synthesis of zinc oxide nanoparticles

Based on the phytochemical screening, ethanol extract was chosen for ZnO NPs synthesis. Defined quantity (2.195 g) of Zinc acetate [$Zn(O_2CCH_3)_2(H_2O)_2$] was weighed and dissolved in 100 mL of Milli-Q-Water and kept in magnetic stirrer for 1 h for complete solubilization. About 80 mL of 0.1 M zinc acetate was added to 20 mL of ethanol leaf extract of *Raphanus sativus* L var. and stirred continuously. During trial, the solution was mixed continuously using a magnetic stirrer. Then, drop wise 2 M NaOH was added with mild stirring then the solution was adjusted to different pH of 8, 10, 12 and 14. Then the solution was heated at 70℃ for 1 h and further stirring was continued using magnetic stirrer for 2 h. The reaction mixture absorbance was measured by UV spectrophotometry (Shimadzu UV-1800 Spectrophotometer) in the wavelength range between 300 and 700 nm to ensure the formation of ZnO NPs. A white crystalline precipitate of ZnO NPs was obtained and it was washed repeatedly with distilled water and checked until pH 7 was obtained. Then, the solution was filtered and dried in a hot air oven at 60 °C [25].

2.5. Biosynthesized ZnO NPs characterization

2.5.1. Optical property of ZnO NPs by UV–vis spectroscopy

To determine the optical property of the synthesized ZnO NPs, small amount of the nanopowder was re-suspended in about 10 mL of de-ionized water and scanned between 300 and 700 nm in UV-Spectrophotometer (Shimadzu UV-1800) and measured the maximum absorbance [25].

2.5.2. Particle size distribution and polydispersity index

The average particle size was measured by Zeta sizer (SZ-100, Horiba scientific, Japan). For the determination of particle size, sterile de-ionized water was used to disperse the nanopowder and sonicated for 10 min for uniform dispersion of nanopowder in the de-ionized water. Dynamic Light Scattering (DLS) of this nanopowder suspension was carried out using Zeta sizer. Based on the function of time, average particle size as hydrodynamic diameter and polydispersity index were measured [37].

2.5.3. FT-IR spectral analysis

Fourier transform infrared (FT-IR) spectroscopy can help in identifying the presence of major functional groups in different phytoconstituents which are associated in the reduction, stabilization and formation of NPs. Surface binding properties of ZnO NPs using *Raphanus sativus* L var. was performed in FT-IR. FT-IR spectrum of the powdered ZnO NPs was obtained by using Bruker Tensor 27 spectrophotometer in Attenuated Total Reflectance (ATR) mode in the spectral range of 4000–400 cm^{-1} with the resolution of 4 cm^{-1}.

2.5.4. Scanning electron microscope

The Scanning electron microscope (SEM) can help in the determination of morphology of ZnO NPs. ZnO NPs morphology was assessed by using SEM (VEGA 3 TESCAN). The synthesized ZnO NPs was prepared as thin film by placing a small volume of synthesized ZnO NPs on the carbon coated copper grid, blotting paper was used to remove the extra solution and the thin film was dried [38].

2.5.5. Transmission electron microscopy (TEM)

For TEM, ZnO NPs was dispersed in aqueous solution (sterile deionized water). This suspension was coated on the carbon-coated copper grid; the sample was allowed to dry. Image of ZnO NPs was analyzed by TEM (JEM-2100, HRTEM, JEOL, JAPAN) at 200 kV as an accelerating voltage.

2.5.6. X-ray diffraction analysis

X-ray diffraction (XRD) of ZnO NPs were analyzed using X-Pert PROPAN with operating current at 30 mA and the voltage at 40 kV. The pattern was recorded by CuK_α radiation. The scanning was done at 2θ from 20 °C to 80 °C [38].

2.6. In vitro *cytotoxicity*

Lung cancer cell line (A549) was utilized to determine the cytotoxic effect of the synthesized ZnO NPs. Cell lines were maintained in a CO_2 incubator with 5% CO_2 at 37 °C [39]. At a concentration of 1×10^3 cells were transferred to 96 well plates and incubated for 24 h. Later, 100 μL of serum-free medium was used to wash the cells and incubated for 1 h in a CO_2 incubator at 37 °C. The cells were treated with ZnO NPs in different concentrations (1–100 μg/mL) and incubated in a CO_2 incubator for 24 h. Wrapped the 96 well plates of cells with aluminum foil to protect from light exposure. At the end of incubation of the well plates, well plate content was removed and 10 μL of the MTT solution (5 mg/mL) was transferred to each well and then incubated at 37 °C in a CO_2 incubator for 5 h. After completion of the incubation period, the MTT solution was removed and about 50μL of Dimethyl sulfoxide (DMSO) was transferred to each well to dissolve the crystals formed. The solution absorbance was recorded in a colorimeter (Shimadzu UV-1800 Spectrophotometer) at 570 nm. Repeated the

experiment in triplicate and the average value were determined. Plotting optical density *vs* ZnO NPs concentration, IC_{50} values were determined.

$$\% \text{ Inhibition} = \frac{[100-\{\text{Absorbance of control}-\text{Absorbance of sample}\}]}{\text{Absorbance of control}} \times 100$$

Following equation was used to express the percentage of cell viability

$$\text{Cell viability} = \frac{\text{Absorbance of control cells}}{\text{Absorbance of treated cells}} \times 100$$

3. Results and discussion

3.1. Phytochemical analysis of Raphanus sativus var. Longipinnatus

Plant origin has huge variety of phytochemicals and has been considered as a bio-active laboratory with multipurpose applications. Hence, these plant origins have importance from ancient time in treating various diseases. In addition, the medicinal plants are cost effective, less side effects, simple effective and easily available. Investigation of phytochemicals in the plant origin can find the approach for its medicinal properties and knowledge of the phytochemicals can establish its medicinal importance leading to discovery and development of a new molecule. The preliminary phytochemical screening test revealed the presence of several phytoconstituents and its results are shown in Table 1 and Fig. 2.

Table 1
Phytochemical analysis of *Raphanus sativus var. Longipinnatus*

	Phytochemical test	Water	Ethanol	DCM
Flavanoid	Alkaline reagent Test	+	+	+
	Lead acetate Test	+	+	+
Alkaloids	Mayer's Test	+	+	+
	Hager's Test	+	+	+
Tannins	Gelatin Test	+	+	+
Phenols		–	+	–
Glycosides		+	+	+
Proteins & Amino Acids		+	+	+
Steroids		–	+	–
Carbohydrates		–	–	–
Saponins		–	+	–
Anthroquinones		–	+	–

+ indicates Presence.
- indicates Absence.

The results revealed that only ethanol extract showed the presence of flavonoids and phenols whereas, phenol was absent in DCM and aqueous extracts. In addition, more number of phytoconstituents in the ethanol extract can be hypothesized to have antioxidant activity and ultimately predicted to have anticancer activity [40,41]. Due to combination of different phytochemicals, plant extract has been considered as a potential alternative one for stabilizing as well as reducing agents in the synthesis of metal nanoparticles [42]. Earlier study results pointed out that phytoconstituents like flavonoids and phenols are responsible for the biosynthesis of metal and metal oxide NPs [43–45]. Our preliminary phytochemical study supported that both flavonoids and phenols are present in the ethanol leaf extract only. Hence, ethanol extract was taken into consideration for feasible ZnO NPs synthesis. Presence of OH groups in flavonoids and phenols can reduce the zinc compounds into ZnO NPs and also act as capping or stabilizing agent of the NPs. Therefore, separate capping or stabilizing agents are not necessary in this synthesis NPs approach [46,47]. In the reduction process, it is hypothesized that zinc acetate acts as the precursor whereas the leaf extracts acts as reducing agent [48].

Reactions involved in the formation of ZnO NPs from zinc acetate are shown as [49].

$$Zn(CH_3COO)_2.2H_2O + 2NaOH \rightarrow Zn(OH)_2 + 2CH_3COONa + 2H_2O \quad (1)$$

$$Zn(OH)_2 + 2H_2O = Zn^{2+} + 2OH^- + 2H_2O = [Zn(OH)_4]^2 \quad (2)$$

$$[Zn(OH)_4]^2 \leftrightarrow ZnO_2^{-2} + 2H_2O \quad (3)$$

$$ZnO_2^{-2} + 2H_2O \leftrightarrow ZnO + 2OH- \quad (4)$$

3.2. Characterization

3.2.1. UV–vis spectra analysis

The UV–vis spectroscopy technique was performed to characterize the optical property and to confirm the formation of ZnO NPs [46]. After addition of zinc acetate with the extract, the resultant white precipitate brings out the key indication of the formation of ZnO NPs. Absorption peaks were not observed at high pH 14 and

Fig. 2. Preliminary Phytochemical Analysis.

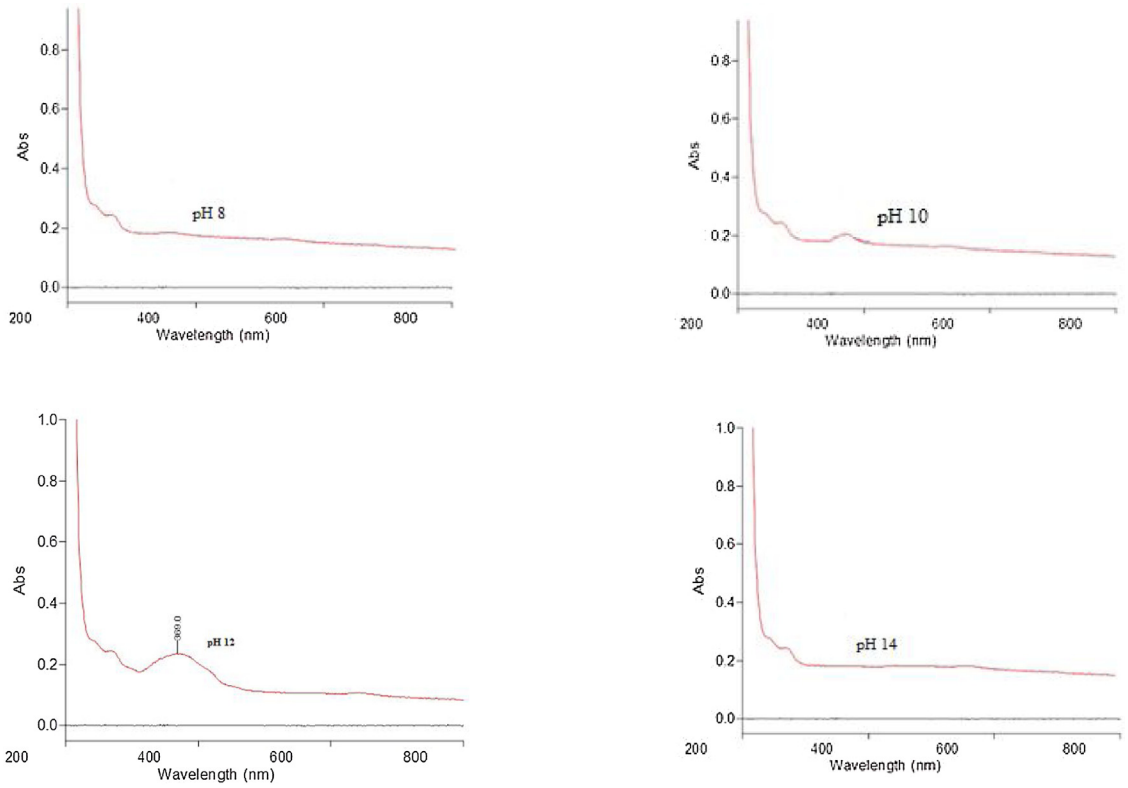

Fig. 3. UV spectra of the ZnO NPs from leaf extract of *Raphanus sativus var. Longipinnatus*.

lower pH between 10 and 8; whereas characteristic peak absorption was observed at 369 nm in pH 12 indicated the reduction of metal oxide and synthesis of ZnO NPs from zinc acetate. Free electrons were present in the ZnO NPs, which has the likelihood to show Surface Plasmon resonance (SPR) absorption band around 370 nm depicting it as an electron-rich metal surface (active surface). Due to electron transitions from valence band to the conduction band (O2p–Zn3d), intrinsic band-gap absorption is observed at 370 nm for ZnO [50,51]. The characteristic peak at 369 nm in the UV region in pH 12 demonstrated that the synthesized NPs are pure ZnO with wurtzite hexagonal phase and the UV spectra of the ZnO NPs are shown in Fig. 3. UV analysis obtained in this study is also on par with the earlier reports [25].

3.2.2. Particle size analysis

DLS method is preferred to analyse the particle size ranging from 5 nm to 5 μm. The average particle size of biozynthesised ZnO NPs was found to be 209 nm. The particle size measurment depends on the several factors such as the type of ions in the medium, the size of surface structures, particle core and particle concentration. Malvern zeta sizer was used for the determination of zeta potential and it was found to be −13.7 mV. The negative sign of the zeta potential value ensures the repulsion between the particles which specifies that the ZnO NPs have good stability. The observed results of particle size and zeta potential are shown in Figs. 4 and 5.

3.2.3. FT-IR spectral analysis

This FT-IR provides information about the molecules vibrational and rotational modes of motion and determines the probable functional groups involved in the formation of ZnO NPs. The observed FTIR spectrum showed (Fig. 6) peaks at 3349, 2781, 1650.98, 1100 and 560 cm^{-1}. The intense and broad peak at 3349 cm^{-1} is associated to H bonded hydroxyl (−OH) group stretching vibration of phenol or alcoholic group [52]; 2781 cm^{-1} is associated to $N-CH_3$ groups with C–H Stretching vibrations; 1650.98 cm^{-1} is associated to carbonyl group (C=O) stretching bands [53]; 1100 cm^{-1} is associated with –C–O–C stretching and

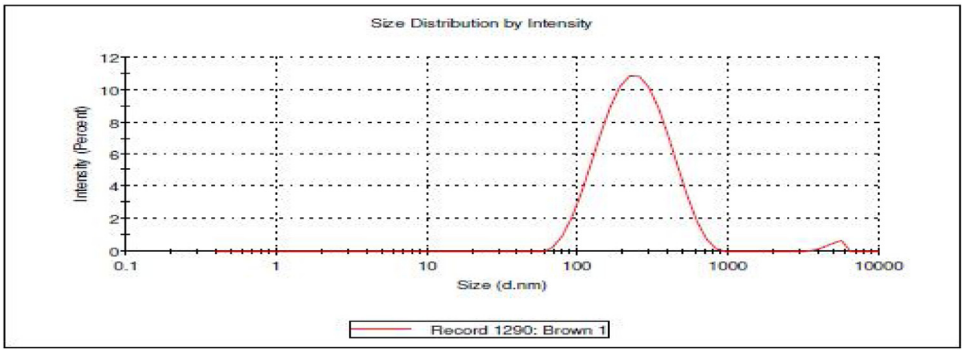

Fig. 4. Particle size analysis of ZnO NPs of leaf extracts of *Raphanus sativus var. Longipinnatus*.

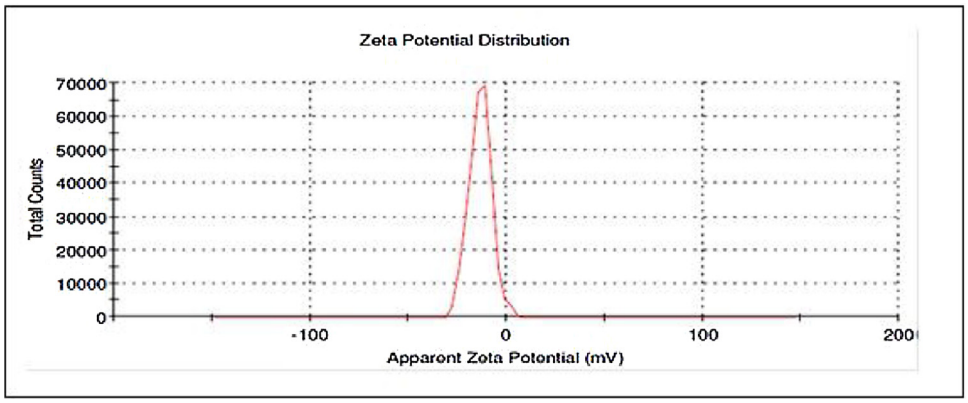

Fig. 5. Zeta potential of the ZnO NPs of leaf extracts of *Raphanus sativus var. Longipinnatus*.

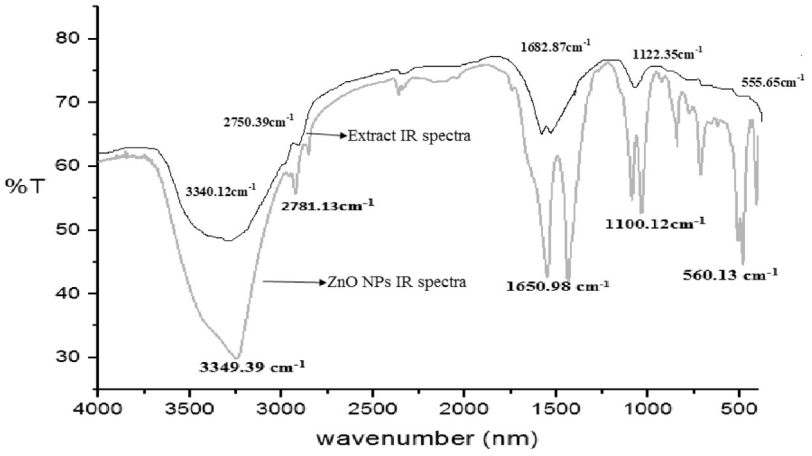

Fig. 6. FTIR spectrum of ZnO NPs of leaf extracts of *Raphanus sativus var. Longipinnatus*.

560 cm^{-1} is the stretching vibration peaks for ZnO denoted as metal oxides (M–O) [54]. The FTIR results showed that there is band shifts either increased or decreased from its original values, this shift in the wavenumber might be due to the presence of different functional groups in the extract.

Presence of flavonoids in the extract plays an important role in the formation of the corresponding metal NPs by reduction of metal ions. The terpenoids are responsible for oxidation of aldehyde groups into carboxylic acid subsequently reduction of metal ions. Presence of flavonoids and terpenoids in the extract play a key role in reduction of metal ions into NPs by active chelation. This is proved by the peak obtained for carbonyl groups (C=O) in the wave number around at 1650.98 cm^{-1}. Reduction of metal ions to NPs has been assumed by a reactive hydrogen atom released from the enol-form to the keto-form due to tautomeric transformations of flavonoids [53].

3.2.4. SEM analysis

SEM analysis is carried out to visualize the NPs size, shape, and surface morphology. SEM VEGA 3 TESCAN model was used in determining the shape of the ZnO NPs in different magnification ranges. The SEM magnification images indicated that the ZnO NPs are spherical, hexagonal shaped NPs with irregular morphology and aggregated NPs. Our study results are comparable with the earlier reports [38]. Biosynthesized ZnO NPs SEM images in different magnifications are shown in Fig. 7.

3.2.5. TEM analysis

Shapes of ZnO NPs were determined by TEM. The TEM image of synthesized ZnO NPs shows different sizes and shapes of the NPs and also outline the aggregation of nanoparticles. The results of DLS method provided larger hydrodynamic diameter of the particle size of NPs. The TEM image of the biosynthesized ZnO NPs is shown in Fig. 8.

3.2.6. XRD analysis

X-ray diffraction has been considered as a non-destructive analytical method which gives the information of different phases, structure and crystal orientation. The diffraction patterns at the 2θ angles of 31.71, 34.41, 36.23, 47.67, 57.61, 62.98, 66.51, 68.05 and 69.21, which were related to lattice plane (100), (002), (101), (102), (110), (103), (200), (112) and (201) respectively. The results prove the hexagonal wurtzite crystal structure of the ZnO NPs. In addition, these Bragg sharp peaks are observed because of the capping agent that stabilized the NPs. Centrifugation process followed by re-dispersion of the formed pellet in Millipore water as purification process ruled out the capping agent's independent crystallization.

Hence, XRD results can recommend the ZnO NPs crystallization. The observed XRD pattern is similar with the Joint Committee on Powder Diffraction Standards (JCPDS) (NO 36-1451) and also on par with the earlier reports [38,55]. X-ray diffraction spectrum of the NPs is shown in Fig. 9.

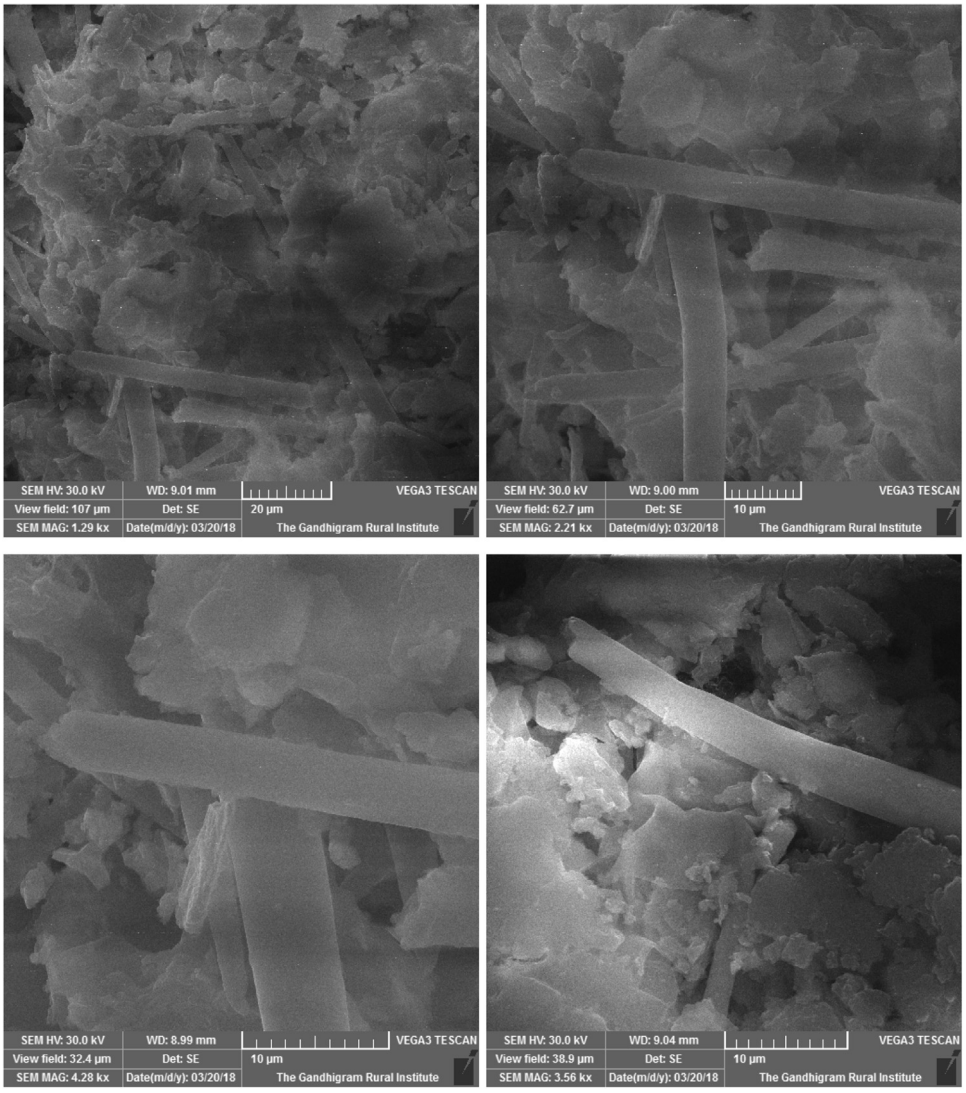

Fig. 7. SEM image of ZnO NPs of leaf extracts of *Raphanus sativus var. Longipinnatus.*

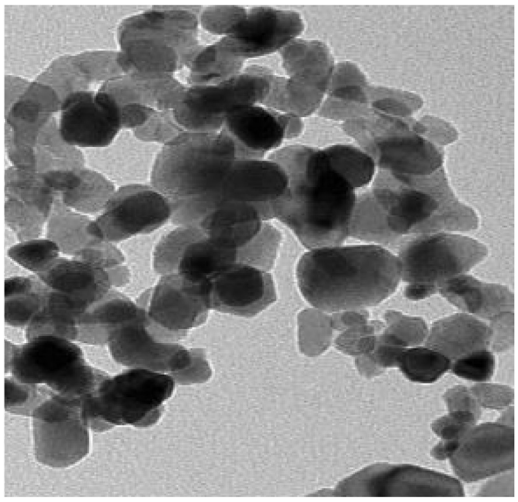

Fig. 8. TEM image of ZnO NPs of leaf extracts of *Raphanus sativus var. Longipinnatus.*

The crystal size of ZnO NPs was calculated by Debye–Scherrer's formula based on the intense peak which is corresponding to (101) plane.

Debye Scherrer's formula

$$D = 0{:}89\ \lambda / (\beta \cos \theta)$$

D is crystal size,

λ is X-ray wavelength, *i.e.* 1.5406 A°

β = FWHM (Full Width at Half Maximum) of the peak located at 2 θ = 36.23° and θ = Bragg's angle of diffraction [55,56].

Based on the Debye Scherrer's formula, the particle size of ZnO NPs was determined to be 66.43 nm. Our XRD study outlined the presence of small particles than the DLS method. Average particle size of the DLS method was found to be about 209 nm which is fairly higher than the X-ray diffraction method, which might be due to smaller nanoparticles agglomeration.

3.2.7. In vitro *cytotoxicity*

The biosynthesized ZnO NPs cytotoxicity was analyzed by *in vitro* technique using A549 cell lines. Cell lines were treated with different concentrations of ZnO NPs (5, 10, 15, 20, 25, 30, 35, 40, 45 and 50 μg mL^{-1}) for 48 h and compared with DMEM as control by the MTT assay. Reduction of MTT reagent and other tetrazolium dyes, changes the yellow color depending upon cellular metabolic activities due to NAD(P)H-dependent cellular oxidoreductase enzymes [57]. After ZnO NPs exposure, in cell viability there were sharp percentage reductions was observed and the IC_{50} was found

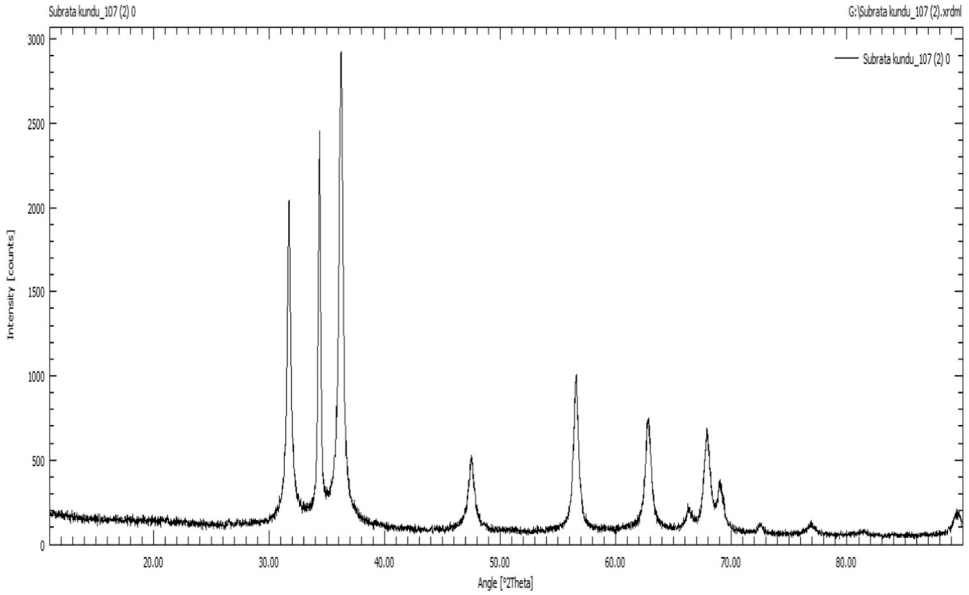

Fig. 9. X- ray diffraction of green synthesized ZnO NPs.

to be 40 μg mL^{-1}. After treating A549 cell line with biosynthesized ZnO NPs, dead cells in high density with changes in morphology were observed; these changes in morphology outlined the cytotoxic enhanced effect. Higher surface area to volume ratio of these small particles may be responsible for enhanced cytotoxic effect. In addition, it is worth mentioning that the presence of phytoconstituents such as anthraquinones and saponins in the ethanolic leaf extract have been considered to exhibit concrete anticancer properties mainly by targeting various cancer-related proteins [58,59].

The possible mechanisms includes DNA damage pathways, paraptosis, autophagy, radiosensitising, overcoming chemoresistance, inhibition of carcinogen-activation of P450 enzymes (phase I metabolism) or induction of carcinogen-detoxifying enzymes (phase II metabolism) or oxidative stress modulation or induction of apoptosis or arresting of the cancer cell cycle [58–60]. Further, research is focused on evaluating its potential mechanism on anticancer activity. From the Fig. 10, the differences among means are statistically significant since the p values are less than 0.0001. The data is expressed in terms of mean ± SD (n = 3).

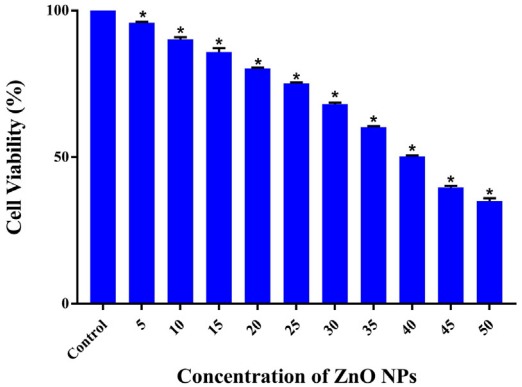

Fig. 10. Anticancer activity of green synthesized ZnO NPs by MTT assay. The data is expressed in terms of mean ± SD (n = 3) *p < 0.0001.

4. Conclusion

The present investigation has proven that the ZnO NPs from *Raphanus sativus var. Longipinnatus* leaf extract is a green synthesis method in solid waste management. Flavonoids and phenols were found as phytoconstituents which played a role as capping or stabilizing agents in the metal NPs synthesis. This protocol has been optimized and provides rapid and large scale up technique for the production of ZnO NPs. This biosynthesized ZnO NPs had a better anti-cancer activity proving that cancer drugs can be prepared by this constituted ecofriendly technique. The study result conclude that the green synthesis of ZnO NPs, using plant material as reducing as well as capping agent, having various merits like easy availability, protection of environmental and economic feasibility in scale up of this process. A thorough understanding of biochemical mechanism in this plant mediated ZnO NPs synthesis is a prerequisite in order to make the approach economically more competitive and sustainable. Process like purification and sterilization technique can provide betterment in green synthesis. In near future, this Nano technological approach will considered as new eco-friendly approach in short span of time.

Declaration of Competing Interest

The authors report no declarations of interest.

References

[1] World Health Organization, Latest Global Cancer Data, (2018) .
[2] F. Mottaghitalab, M. Farokhi, Y. Fatahi, F. Atyabi, R. Dinarvand, J. Control. Release 295 (2019) 250–267.
[3] T.V.M. Sreekanth, P.C. Nagajyothi, P. Muthuraman, G. Enkhtaivan, S.V.P. Vattikuti, C.O. Tettey, et al., J. Photoche. Photobiol. B: Biol. 188 (2018) 6–11.
[4] N.Z. Msomi, M.B.C. Simelane, Herbal Medicine, InTech, Croatia, 2018, pp. 215–227.
[5] C. Mason, S. Vivekanandhan, M. Misra, A.K. Mohanty, World J. Nano Sci. Eng. 2 (2012) 47–52.
[6] N. Sangeeth, A.K. Kumaraguru, Nanobiotechnol. 11 (2013) 1–11.
[7] T. Klaus-Joerger, R. Joerger, E. Olsson, C. Granqvist, Trends Biotechnol. 19 (2001) 15–20.
[8] K.C. Bhainsam, S.F.D. Souza, Colloids Surf. B Biointerfaces 47 (2006) 160–164.
[9] A. Ahmad, S. Senapati, M.I. Khan, R. Kumar, M. Sastry, Langmuir 19 (2003) 3550–3553.
[10] N. Krithiga, A. Rajalakshmi, A. Jayachitra, J. Nanosci. (2015) Article ID 928204.

[11] S. Ahmed, M. Ahmad, B.L. Swami, S. Ikram, J. Adv. Res. 7 (2016) 17–28.
[12] S.Jain.M.S. Mehata, Sci. Rep. 7 (2017) 15867.
[13] H.F. Aritonang, H. Koleangan, A.D. Wuntu, Int. J. Microbio. (2019) Article ID 8642303.
[14] K.S. Kavitha, B. Syed, D. Rakshith, H.U. Kavitha, H.C.Y. Rao, B.P. Harini, et al., Int. Res. J. Biological Sci. 2 (2013) 66–76.
[15] S. Iravani, Green Chem. 13 (2011) 2638–2650.
[16] A. Eslami, M.M. Amjini, A.R. Yazdanbakhsh, A.M. Bandpei, A.A. Safari, A. Asadi, J. Chem. Technol. Biotechnol. 91 (2016) 2693–2704.
[17] B.T. Sone, E. Manikandan, A.G. Fakim, M. Maaza, J. Alloys. Compd. 650 (2015) 357–362.
[18] B.T. Sone, E. Manikandan, A.G. Fakim, M. Maaza, Green Chem. Lett. Rev. 9 (2016) 85–90.
[19] F.T. Thema, E. Manikandan, A.G. Fakim, M. Maaza, J. Alloys. Compd. 657 (2016) 655–661.
[20] N. Thovhogi, E. Park, E. Manikandan, M. Maaza, A.G. Fakim, J. Alloys. Compd. 655 (2016) 314–320.
[21] A. Diallo, B.M. Mothudi, E. Manikandan, M. Maaza, J. Nanophotonics 10 (2016) 26010.
[22] A. Diallo, E. Manikandan, V. Rajendran, M. Maaza, J. Alloys. Compd. 681 (2016) 561–570.
[23] O. Długosz, J. Chwastowski, M. Banach, Chem. Pap. 74 (2020) 239–252.
[24] G. Asab, E.A. Zereffa, T.A. Seghne, Int. J. Biomater. (2020)4783612.
[25] P. Jamdagni, P. Khatri, J.S. Rana, JKSUS 30 (2018) 168–175.
[26] U. Ozgur, Ya.I. Alivov, C. Liu, A. Teke, M.A. Reshchikov, S. Dogan, et al., J. Appl. Phys. 98 (2005) 041301.
[27] M. Ramesh, M. Anbuvannan, G. Viruthagiri, Spectrochim. Acta Part A. 136 (2015) 864–870.
[28] J. Jiang, J. Pi, J. Cai, Bioinorg. Che. Appl. (2018)1062562.
[29] R. Dobrucka, J. Dugaszewska, Saudi J. Biol. Sci. 23 (2016) 517–523.
[30] J. Santhoshkumar, S. Venkat Kumar, S. Rajeshkumar, Resour. Technol. 3 (2017) 459–465.
[31] G. Bhumi, N. Savithramma, Int. J. Drug Dev. Res. 6 (2014) 208–214.
[32] G. Sundaraselvan, S. Darlin Quine, J. Nanosci. Tech. 3 (2017) 289–292.
[33] K.K. Panda, D. Golari, A. Venugopal, V.M.M. Achary, G. Phaomei, N.L. Parinandi, et al., Antioxidants 6 (2017) 35.
[34] K. Ali, S. Dwivedi, A. Azam, Q. Saquib, M.S. Al-Said, A. Alkhedhairy, et al., J. Colloid Interface Sci. 472 (2016) 145–156.
[35] R.M. Gutierrez, R.L. Perez, ScientificWorld J. 4 (2004) 817–837.
[36] C.K. Kokate, A.P. Purohit, S.B. Gokhale, Pharmacognosy, 47th edn., Nirali Prakashan Publication, India, 2011.
[37] A.A. Ashour, D.R.H.M. El-Gowelli, A. HEl-Kamel, Int. J. Nanomed. Nanosurg. 10 (2015) 7207–7221.
[38] T.S. Anvekar, V.R. Chari, H. Kadam, Mat. Sci. Res. India. 14 (2017) 153–157.
[39] A. Bahuguna, I. Khan, V.K. Bajpai, S.C. Kang, Bangladesh J. Pharmacol. 12 (2017) 115–118.
[40] E. Middleton, C. Kandaswami, T.C. Theoharides, Pharmacol. Rev. 52 (2000) 673–751.
[41] A. Doss, Anc. Sci. Life 29 (2009) 12–16.
[42] S. Ahmed, M. Ahmad, B.L. Swami, S. Ikram, J. Adv. Res. 7 (2016) 17–28.
[43] F. Luo, D. Yang, Z.L. Chen, M. Megharaj, R. Naidu, J. Hazard. Mater. 303 (2016) 145–153.
[44] A.K. Mittal, Y. Chisti, U.C. Banerjee, Biotechnol. Adv. 31 (2013) 346–356.
[45] X. Weng, M. Guo, F. Luo, Z. Chen, Chem. Eng. J. 308 (2017) 904–911.
[46] N. Senthilkumar, E. Nandhakumar, P. Priya, D. Soni, M. Vimalan, I. Vetha Potheher, New J.Chem. 41 (2017) 10347.
[47] K. Aoki, J. Chen, N. Yang, H. Nagasava, Langmuir 19 (2003) 9904–9905.
[48] A. Happy, M. Soumya, S. Venkat Kumar, S. Rajeshkumar, R. David Sheba, T. Lakshmi, et al., Bioche. Biophy. Rep. 17 (2019) 208–211.
[49] A. Umamaheswari, S. Lakshmana Prabu, A. Puratchikody, MOJ Bioequiv Availab. 5 (2018) 151–154.
[50] A. Khorsand Zak, R. Yousefi, W.H.A. Majid, M.R. Muhamad, Ceram. Int. 38 (2012) 2059–2064.
[51] M.K. Kavitha, H. John, P. Gopinath, R. Philip, J. Mater. Chem. C Mater. Opt. Electron. Devices 23 (2013) 3669–3676.
[52] A.M. Awwad, Salem N.M, A.O. Abdeen, Int. J. Ind. Chem. Biotechnol. 4 (2013) 29.
[53] L. Rastogi, J. Arunachalam, Mater. Chem. Phys. 129 (2011) 558–563.
[54] R. Yuvakkumar, J. Suresh, B. Saravanakumar, A.J. Nathanaeld, S.I. Hong, V. Rajendran, Spectrochim. Acta Part A Mol. Biomol. Spectrosc. 137 (2015) 250–258.
[55] S. Talam, S.R. Karumuri, N. Gunnam, ISRN Nanotechnol. (2012)372505.
[56] R. Vijayalakshmi, V. Rajendran, Arch. Appl. Sci. Res. 4 (2012) 1183–1190.
[57] M.V. Berridge, P.M. Herst, A.S. Tan, Biotechnol. Annu. Rev. 11 (2005) 127–152.
[58] W. Tian, C. Wang, D. Li, H. Hou, Future Med. Chem. 12 (2020) 627–644.
[59] X.X. Huang, L. Ting, C.M.V. Fong, X. Chen, X.J. Chen, Y.T. Wang, et al., Molecules 21 (2016) 1326.
[60] P. Piman, W. Natthida, T. Waraporn, T. Kanjana, Asian Pac. J. Trop. Biomed. 7 (2017) 998–1004.